From rocksalt to perovskite: a metathesis route for the synthesis of perovskite oxides of current interest

Tapas Kumar Mandal and J. Gopalakrishnan*

Solid State and Structural Chemistry Unit, Indian Institute of Science, Bangalore 560 012, India. E-mail: gopal@sscu.iisc.ernet.in

Solid state metathesis reactions between lithium containing rocksalt metal oxides and appropriate lanthanum/ alkaline earth metal oxychloride/chloride provide a convenient route for the synthesis of several perovskite oxides of current interest, such as $LaCoO_3$, $LaMnO_3$, $AMnO_3$ and $ATiO_3$ (A = Ca, Sr, Ba). Similarly, metathesis reactions between Li_2TiO_3/Li_2ZrO_3 and $PbSO_4$ (instead of $PbCl_2$) yield $PbTiO_3$, $PbZrO_3$ and $PbZr_{1-x}Ti_xO_3$ perovskites. $BaPbO_3$ and superconducting $BaPb_{0.75}Bi_{0.25}O_3$ could also be synthesized by the metathesis reaction between $Li_2PbO_3/Li_2(Pb,Bi)O_3$ and $Ba(OH)_2 \cdot 8H_2O$. Uniformly in all cases, the perovskite oxides were obtained in the form of loosely connected submicron sized particles at considerably lower temperatures than those usually employed for their synthesis by ceramic methods.

Introduction

Synthesis of perovskite oxides continues to attract research attention, because realization of newer/technologically important properties requires the materials to be produced in a special morphology, for example, as thin films, porous solids, monodisperse particles, free standing particles of nanometer dimensions and so on. Conventional synthetic methods involving high temperature solid state reactions (ceramic method) are of no avail for this purpose. Therefore materials chemists constantly endeavour to develop novel methods that enable them to assemble/synthesize perovskite oxides under mild conditions to achieve the desired morphology/structure/properties. For example, pulsed laser deposition of films stabilizes the metastable perovskite structure, instead of the stable hexagonal form for $YMnO_3$.[1] Fine particles of $BaTiO_3$ and highly crystalline ferromagnetic (T_c = 330 K) $La_{0.5}Ba_{0.5}MnO_3$ with narrow particle size distribution (~ 0.5 μm) are obtained by subcritical solvo/hydrothermal synthesis at surprisingly low temperatures (80–240 °C).[2,3] Similarly a special sol–gel method employing single bimetallic alkoxide precursor $[BaTi(O_2\text{-}CC_7H_{15})[OCH(CH_3)_2]_5]$ has been developed to produce monodisperse nanoparticles (6–12 nm) of $BaTiO_3$.[4] The sol–gel route has also been adapted to synthesize free-standing nanoparticles (10–30 nm) of ferroelectric $Pb(Zr_{0.5}Ti_{0.5})O_3$ (PZT).[5] Submicron $PbZrO_3$ powders have been made at relatively low temperatures in a solid state reaction of $PbSO_4$, ZrO_2 and K_2CO_3 followed by leaching out of K_2SO_4 in water.[6] La_2CuO_4 with a high surface area and enhanced oxygen mobility has been prepared by a new method involving hydrolysis of metal acetates in supercritical water (> 374 °C).[7]
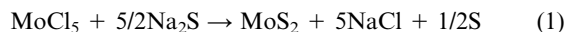
Solid state metathesis (SSM) reactions[8] provide a convenient route for the synthesis of a wide variety of non-oxide ceramic

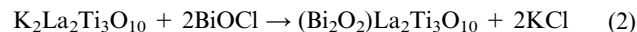**Table 1** Synthesis of perovskite oxides by metathesis

Reaction	Conditions	Perovskite oxide
$LiCoO_2 + LaOCl \rightarrow LaCoO_3 + LiCl$	810 °C/12 h/air	$LaCoO_3$[a]: rhombohedral (R-$3c$); a_h = 5.442(1) Å; c_h = 13.093(1) Å
$LiMnO_2 + LaOCl + x/2O_2 \rightarrow LaMnO_{3+x} + LiCl$	850 °C/12 h/air	$LaMnO_{3+x}$[b]: orthorhombic ($Pnma$); a = 5.495(6) Å; b = 7.774(6) Å; c = 5.503(3) Å
$LiMnO_2 + LaOCl \rightarrow LaMnO_3 + LiCl$	850 °C/12 h/argon	$LaMnO_3$[c]: orthorhombic ($Pbnm$); a = 5.535(3) Å; b = 5.747(1) Å; c = 7.702(3) Å
$Li_2MnO_3 + CaCl_2 \rightarrow CaMnO_3 + 2LiCl$	850 °C/12 h/air	$CaMnO_3$[d]: orthorhombic ($Pnma$); a = 5.275(2) Å; b = 7.442(10) Å; c = 5.273(7) Å
$Li_2MnO_3 + SrCl_2 \rightarrow SrMnO_3 + 2LiCl$	810 °C/12 h/air	$SrMnO_3$[e]: hexagonal-4H ($P6_3/mmc$); a = 5.452(1) Å; c = 9.081(1) Å
$Li_2MnO_3 + BaCl_2 \rightarrow BaMnO_3 + 2LiCl$	850 °C/12 h/air	$BaMnO_3$[f]: hexagonal-2H ($P6_3/mmc$); a = 5.703(1) Å; c = 4.815(1) Å
$Li_2TiO_3 + CaCl_2 \rightarrow CaTiO_3 + 2\ LiCl$	900 °C/12 h/air	$CaTiO_3$[g]: orthorhombic ($Pnma$); a = 5.438(1) Å; b = 7.643(3) Å; c = 5.377(2) Å
$Li_2TiO_3 + SrCl_2 \rightarrow SrTiO_3 + 2\ LiCl$	900 °C/12 h/air	$SrTiO_3$[h]: cubic ($Pm3m$); a = 3.903(1) Å
$Li_2TiO_3 + BaCl_2 \rightarrow BaTiO_3 + 2\ LiCl$	900 °C/24 h/air	$BaTiO_3$[i]: tetragonal ($P4/mmm$); a = 3.992(1) Å; c = 4.034(2) Å
$Li_2TiO_3 + PbSO_4 \rightarrow PbTiO_3 + Li_2SO_4$	810 °C/12 h/air	$PbTiO_3$[j]: tetragonal ($P4mm$); a = 3.900(1) Å; c = 4.144(1) Å
$Li_2ZrO_3 + PbSO_4 \rightarrow PbZrO_3 + Li_2SO_4$	810 °C/6 h/850 °C/6 h/air	$PbZrO_3$[k]: orthorhombic ($P2cb$); a = 8.230(4) Å; b = 11.784(8) Å; c = 5.885(3) Å
$Li_2PbO_3 + Ba(OH)_2 \rightarrow BaPbO_3 + 2\ LiOH$	510 °C/6 h/air	$BaPbO_3$[l]: cubic ($Pm3m$); a = 4.274(1) Å

[a] JCPDS 25–1060. [b] Ref. 24. [c] Ref. 25. [d] Ref. 27. [e] JCPDS 24–1213. [f] JCPDS 26–0168. [g] JCPDS 42–0423. [h] JCPDS 35–0734. [i] JCPDS 05–0626. [j] JCPDS 06–0452. [k] JCPDS 35–0739. [l] JCPDS 12–0664.

materials such as borides, carbides, silicides, pnictides and chalcogenides.[9–11] A typical SSM reaction, for example,
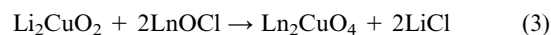
$$MoCl_5 + 5/2Na_2S \rightarrow MoS_2 + 5NaCl + 1/2S \qquad (1)$$

involves exchange of atomic/ionic species between the reactants to give stable products, accompanied by a large enthalpy change (ΔH_m) and high adiabatic reaction temperature (T_m). Thus, for reaction (1), ΔH_m and T_m are -890 kJ mol^{-1} and 1413 °C respectively. The reactions are often self-propagating and believed to be driven by the formation of stable salt byproducts such as alkali halides with a high lattice energy.[10] In our laboratory, we have developed a different metathesis route[12,13] for the synthesis of perovskite-related oxides, a typical example being

$$K_2La_2Ti_3O_{10} + 2BiOCl \rightarrow (Bi_2O_2)La_2Ti_3O_{10} + 2KCl \qquad (2)$$

Here layered units, $[Bi_2O_2]^{2+}$ and $[La_2Ti_3O_{10}]^{2-}$, retain their structural identity during the metathesis, enabling the assembly of new layered perovskites. A major difference between metathesis reactions (1) and (2) is that unlike (1), reaction (2) is not self-propagating and requires longer duration (6–12 h) at temperatures closer to/higher than the melting point of the coproduced salt.

We have employed a similar metathesis reaction[14] between Li_2CuO_2 and LnOCl (Ln = La, Nd)

$$Li_2CuO_2 + 2LnOCl \rightarrow Ln_2CuO_4 + 2LiCl \qquad (3)$$
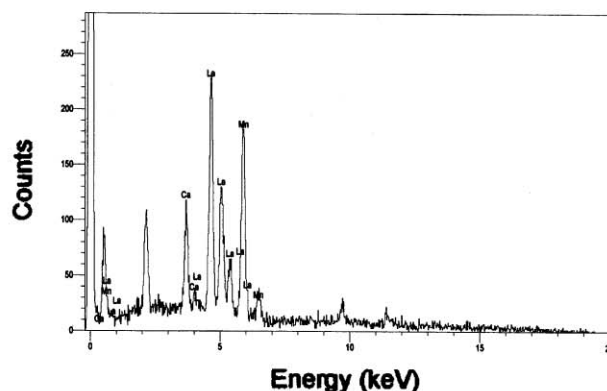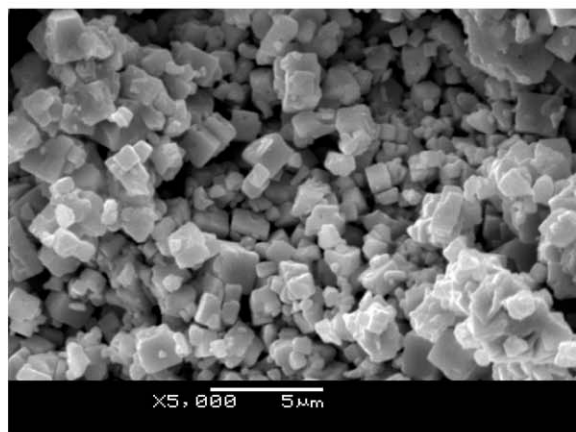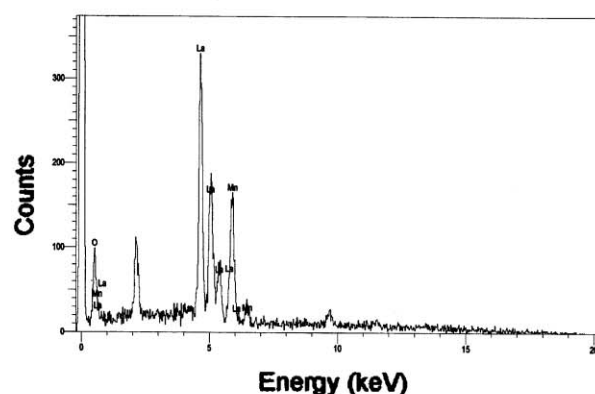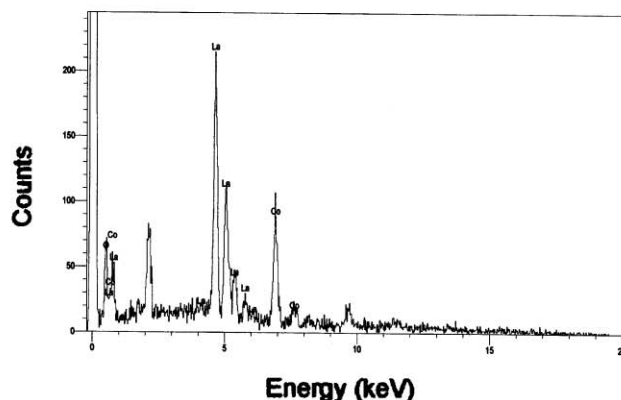
for the synthesis of La_2CuO_4/Nd_2CuO_4 as well as the

Fig. 1 (Left) SEM pictures of $LaCoO_3$ (top), $LaMnO_{3+x}$ (middle) and $La_{2/3}Ca_{1/3}MnO_3$ (bottom). The corresponding EDX spectra are shown on the right side panels.
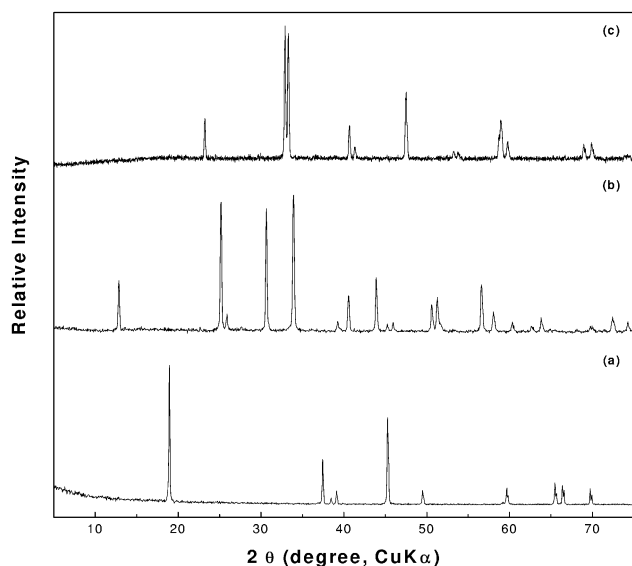
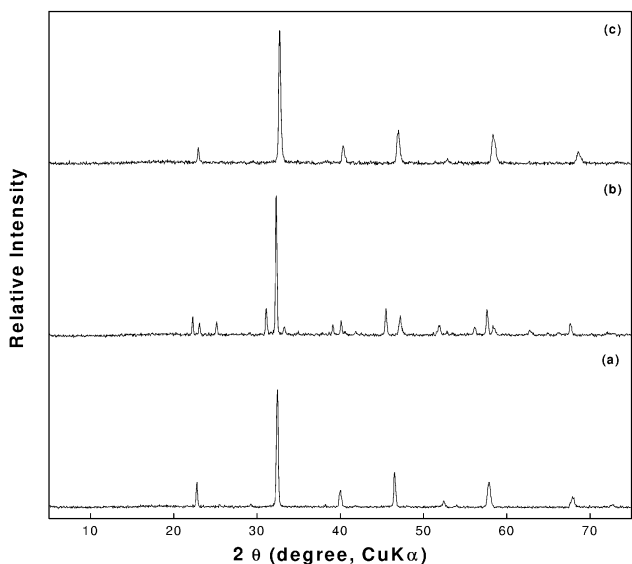**Fig. 2** Powder XRD patterns of (a) $LiCoO_2$, (b) LaOCl and (c) $LaCoO_3$.

Fig. 3 Powder XRD patterns of (a) $LaMnO_{3+x}$, (b) $LaMnO_3$ and (c) $La_{2/3}Ca_{1/3}MnO_3$.
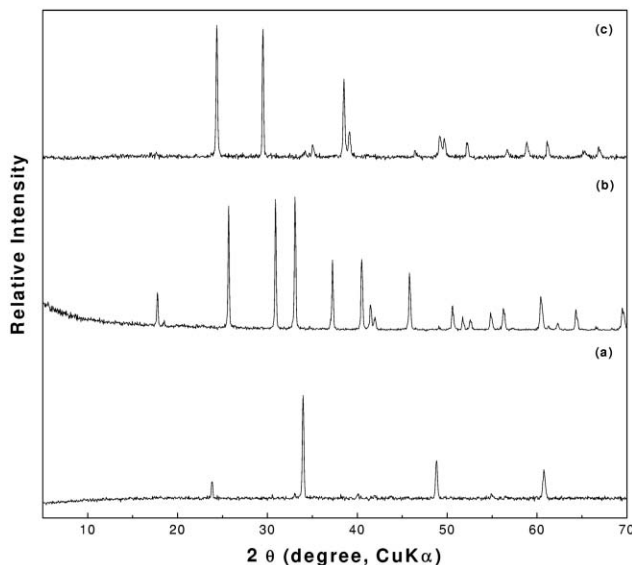

Fig. 4 Powder XRD patterns of (a) $CaMnO_3$, (b) $SrMnO_3$ and (c) $BaMnO_3$.
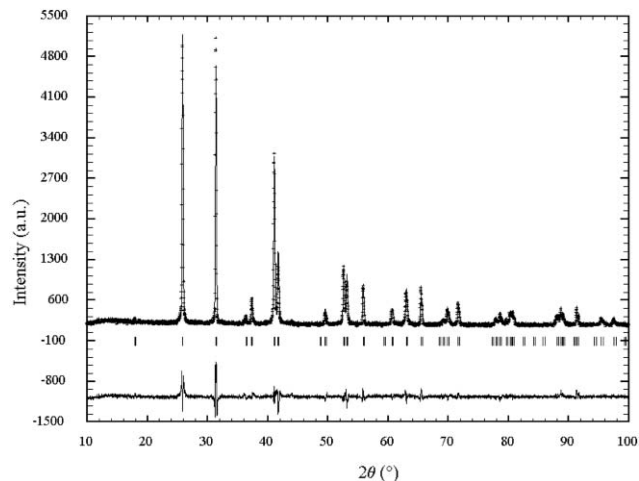

Fig. 5 Rietveld refinement of the structure of $BaMnO_3$ from powder XRD data. Observed (+), calculated (—) and difference (bottom) profiles are shown.

Table 2 Atomic positions, occupancy and isotropic thermal parameters for $BaMnO_3^a$

Atom	Wy	x	y	z	$B/Å^2$	Occupancy
Ba	2d	0.333	0.667	0.75	2.04(5)	1.0
Mn	2a	0.0	0.0	0.0	2.41(1)	1.0
O	6h	0.131(1)	0.290(1)	0.25	0.43(1)	1.0

^{a} Space group, $P6_3/mmc$, $a = 5.700(1)$, $c = 4.814(1)$ Å, $\gamma = 120°$, $R_{Bragg} = 6.8\%$, $R_f = 6.0\%$, $R_p = 7.6\%$, $R_{wp} = 10.2\%$, $R_{exp} = 6.1\%$ and $\chi^2 = 2.62$.

Fig. 6 Powder XRD patterns of (a) $CaTiO_3$, (b) $SrTiO_3$ and (c) $BaTiO_3$.

superconducting analogues, where the lithium-containing oxide, Li_2CuO_2, serves as a convenient precursor for formation of the desired product. Several rocksalt related metal oxides are known[15,16] (e.g. $LiMnO_2$, $LiCoO_2$, Li_2TiO_3, Li_2MnO_3, Li_2ZrO_3 and Li_2PbO_3) which could serve as precursors for the synthesis of the corresponding perovskite oxides (e.g. $LaMnO_3$, $LaCoO_3$, $BaTiO_3$, $PbTiO_3$, $BaMnO_3$, $PbZrO_3$ and $BaPbO_3$) in similar metathesis reactions. We explored this possibility at some length and found that, by a suitable choice of the reaction partner [LaOCl, ACl_2 (A = Ca, Sr, Ba), $PbSO_4$ and $Ba(OH)_2$], we could synthesize several of the perovskite oxides of current interest. Our investigations have also provided new insight into

Fig. 7 Rietveld refinement of the structure of BaTiO$_3$. Observed (+), calculated (—) and difference (bottom) profiles are shown.

Table 3 Atomic positions, occupancy and isotropic thermal parameters for tetragonal BaTiO$_3^a$

Atom	Wy	x	y	z	$B/\text{Å}^2$	Occupancy
Ba	1a	0.0	0.0	0.0	1.32(1)	1.0
Ti	1b	0.5	0.5	0.522(3)	0.99(1)	1.0
O1	1b	0.5	0.5	−0.010(2)	0.75(2)	1.0
O2	2c	0.5	0.0	0.434(3)	0.65(1)	1.0

[a] Space group $P4/mmm$, $a = 3.9959(1)$, $c = 4.0358(1)$ Å, $R_{\text{Bragg}} = 7.8\%$, $R_f = 5.8\%$, $R_p = 10.2\%$, $R_{wp} = 13.3\%$, $R_{\text{exp}} = 8.9\%$ and $\chi^2 = 2.24$.
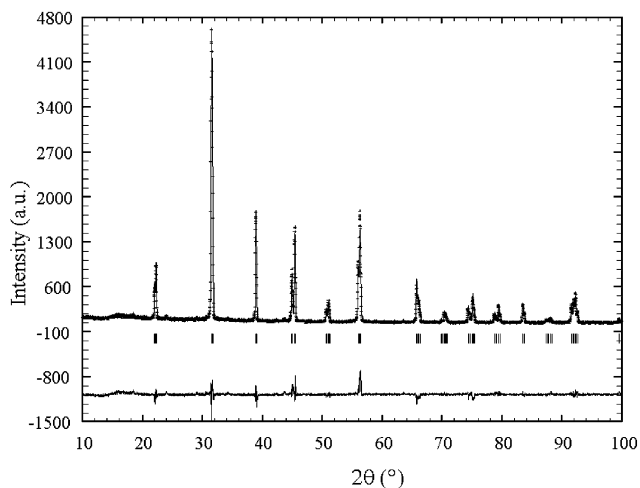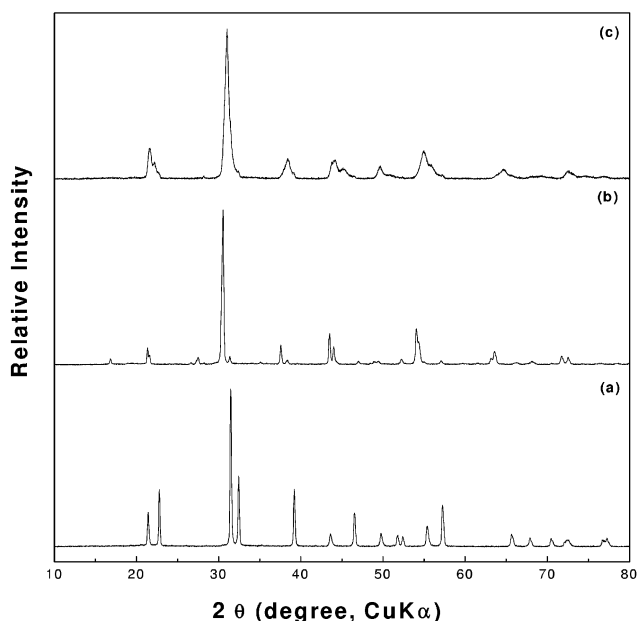

Fig. 8 Powder XRD patterns of (a) PbTiO$_3$, (b) PbZrO$_3$ and (c) PbZr$_{0.5}$Ti$_{0.5}$O$_3$.

the thermodynamics of these metathesis processes. The results are described in this paper.

Experimental

Synthesis

The starting materials, Li$_2$MO$_3$ (M = Ti, Mn, Zr and Pb), LiMO$_2$ (M = Mn, Co) and LaOCl were prepared using high
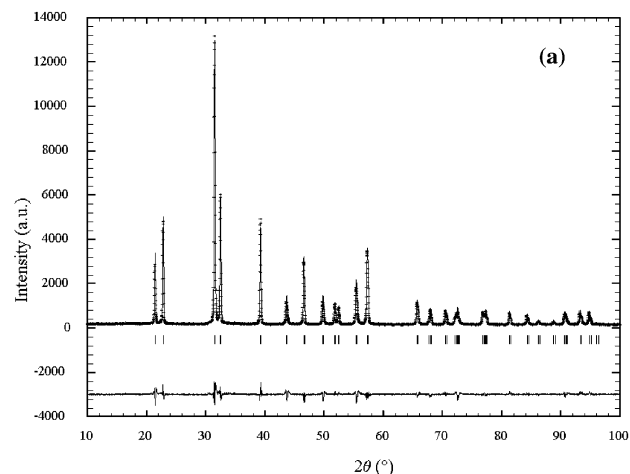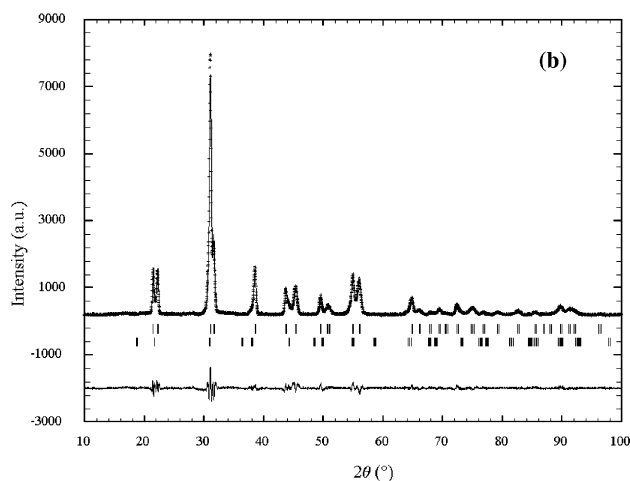

Fig. 9 Rietveld refinement of the structures of (a) PbTiO$_3$ and (b) PbZr$_{0.48}$Ti$_{0.52}$O$_3$. Observed (+), calculated (—) and difference (bottom) profiles are shown.

purity (>99%) components. Li$_2$TiO$_3$ and Li$_2$ZrO$_3$ were prepared[17,18] by reacting stoichiometric quantities of Li$_2$CO$_3$ and TiO$_2$/ZrO$_2$ at 1000 °C for 24 h in air. Li$_2$MnO$_3$, similar to the one reported by Paik *et al.*,[19] was prepared by reacting LiOH·H$_2$O and MnC$_2$O$_4$·2H$_2$O at 400 °C for 12 h and 600 °C for 12 h in air with intermediate grindings. Li$_2$PbO$_3$ was prepared from Li$_2$CO$_3$ and PbO$_2$ at 600 °C/12 h and 660 °C/6 h in flowing oxygen. LiCoO$_2$ and LiMnO$_2$ were prepared by reacting Li$_2$CO$_3$ with MC$_2$O$_4$·2H$_2$O (M = Co, Mn) at elevated temperatures. For LiMnO$_2$, a final anneal in argon at 1020 °C for 24 h was required to obtain a phase-pure sample. LaOCl was prepared[20] by reacting La$_2$O$_3$ (predried at 900 °C) with an equal quantity of NH$_4$Cl at 300, 500 and 900 °C for 2–4 h at each temperature. Purity of the phases in all cases was

Table 4 Atomic positions, occupancy and isotropic temperature factors for PbZr$_{0.48}$Ti$_{0.52}$O$_3^{a,b}$

Tetragonal (Phase fraction ~ 90 ± 2%)						
Atom	Wy	x	y	z	$B/\text{Å}^2$	Occupancy
Pb	1a	0.0	0.0	0.0	1.24(7)	1.0
Ti	1b	0.5	0.5	0.546(1)	0.66(1)	0.52
Zr	1b	0.5	0.5	0.546(1)	0.65(1)	0.48
O1	2c	0.5	0.0	0.596(3)	0.88(1)	1.0
O2	1b	0.5	0.5	0.097(4)	0.85(1)	1.0

[a] Space group $P4mm$, $a = 3.999(1)$, $c = 4.141(1)$ Å, $R_{\text{Bragg}} = 3.3\%$, $R_f = 2.5\%$, $R_p = 10.2\%$, $R_{wp} = 13.3\%$, $R_{\text{exp}} = 8.9\%$ and $\chi^2 = 2.24$. [b] Rhombohedral (phase fraction ~ 10 ± 2%); Space group $R3m$, $a = 5.779(1)$, $c = 14.218(4)$ Å, $\gamma = 120°$.

ascertained by powder X-ray diffraction (XRD) and comparison with standard diffraction data files (JCPDS).

Formation of perovskite oxides by metathesis was investigated by reacting the lithium-containing rocksalt precursor oxides with appropriate metal halide, oxyhalide or sulfate in the solid state at elevated temperatures. The products were examined by XRD at various stages to determine conditions for the formation of single-phase materials. At the final stage, the products were washed with distilled water and dried. The synthesis conditions together with characterization of the perovskite oxides formed in the metathesis reactions are summarized in Table 1.

Characterization

Powder XRD patterns were recorded using a SIEMENS D5005 X-ray powder diffractometer (Cu Kα radiation). Lattice parameters of the single-phase products were refined by least-squares refinement of the powder diffraction data using the PROSZKI[21] program. In selected cases, the structures were refined by Rietveld refinement of the powder XRD data using the FULLPROF[22] program. For refinement, XRD data were collected in the 2θ ranges 10–100° with a step size of 0.02° using a 5 s/step scan speed. Scanning electron microscopy (SEM) and energy dispersive X-ray analysis (EDX) were carried out using a JEOL-JSM-5600 LV microscope at a 20 kV accelerating
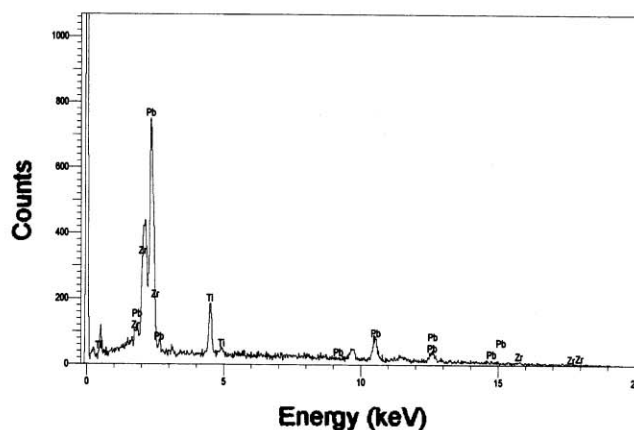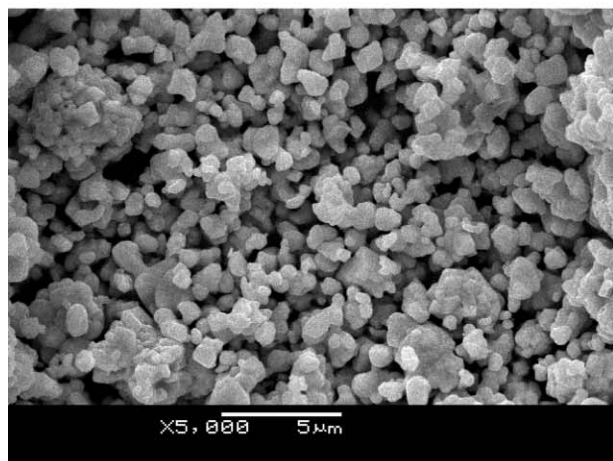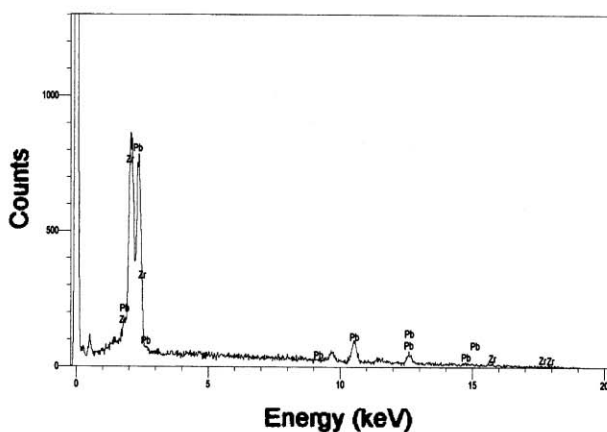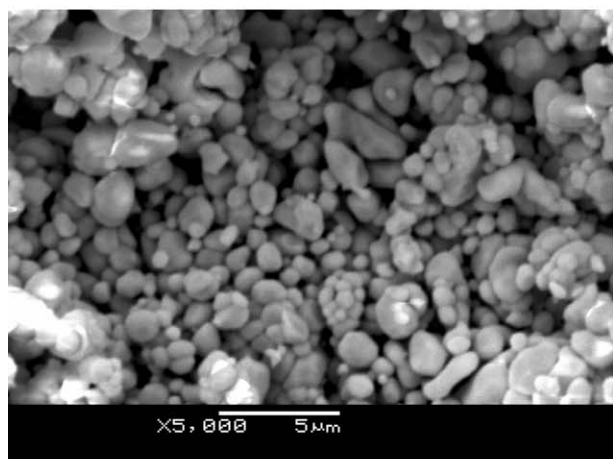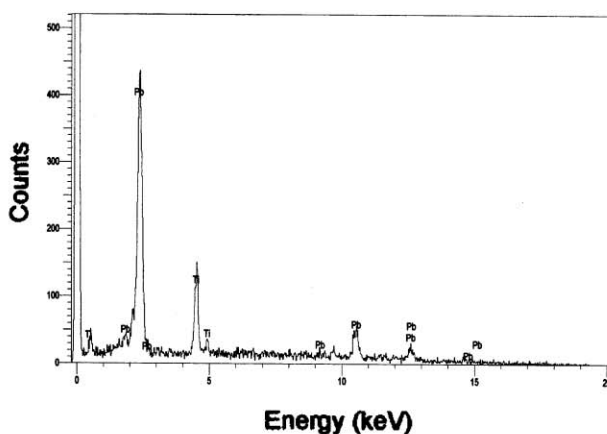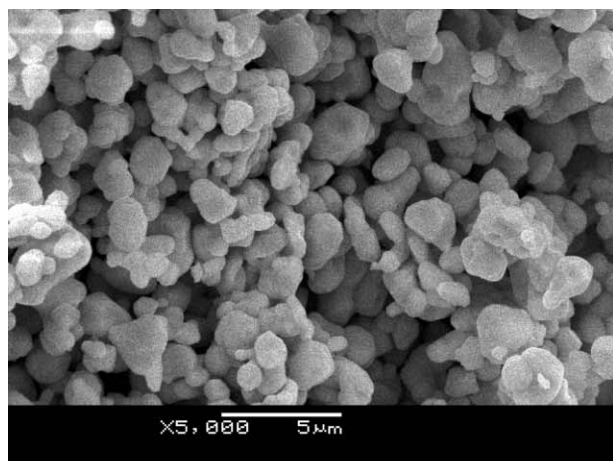

Fig. 10 (Left) SEM pictures of $PbTiO_3$ (top), $PbZrO_3$ (middle) and $PbZr_{0.48}Ti_{0.52}O_3$ (bottom). The corresponding EDX spectra are shown on the right side panels.

voltage fitted with a Be window detector. The oxidation state of manganese in stoichiometric $LaMnO_3$ as well as the Mn^{III}/Mn^{IV} ratios in $LaMnO_{3 + \delta}$ and $La_{2/3}Ca_{1/3}MnO_3$ was determined by iodometric titration[23] using KI.
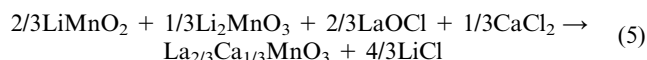
Results and discussion

Considering that lithium containing solids (*e.g.* Li_3N, Li_2S, Li_2CuO_2) constitute convenient precursors in metathesis reactions,[9,11,14] we investigated the possibility of developing metathesis as a general route for the synthesis of perovskite (ABO_3) oxides starting from lithium containing rocksalt precursor oxides.[15,16] For this purpose, we first investigated the reaction of rocksalt oxides, $LiCoO_2$ and $LiMnO_2$, with LaOCl. The metathesis

$$LiCoO_2 + LaOCl \rightarrow LaCoO_3 + LiCl \quad (4)$$

occurs readily around 810 °C (Table 1) yielding directly the well-known $LaCoO_3$ perovskite. After washing out the LiCl byproduct, we see that the product $LaCoO_3$ is single-phase submicron sized crystals with clean grain boundaries (Fig. 1, top). The powder XRD pattern (Fig. 2) shows that the product is free from starting materials ($LiCoO_2$ and LaOCl). EDX analysis of the washed product showed the absence of chloride impurity. Lattice parameters derived from the XRD data are in agreement with the values reported for rhombohedral (R-3c) $LaCoO_3$ (Table 1). Similarly we could synthesize $LaMnO_3$ around 850 °C by the metathesis reaction between $LiMnO_2$ and LaOCl (Table 1). Here, we have been able to synthesize both stoichiometric ($LaMnO_3$) and nonstoichiometric ($LaMnO_{3 + x}$; $x \sim 0.08$) phases by carrying out the metathesis reaction in flowing argon and air respectively. Powder XRD patterns of both $LaMnO_3$ and $LaMnO_{3 + x}$ phases are in agreement with the data reported in the literature[24,25] (Fig. 3, Table 1). It must be mentioned that both $LaCoO_3$ and $LaMnO_3$ are synthesized by the metathesis route at relatively low temperatures (800–850 °C) as compared to their synthesis by conventional means (>1000 °C). In addition, the particle size (<1 μm) and their interconnectivity (Fig. 1) are different from those obtained in conventional high temperature synthesis.

We could also synthesize readily the magnetoresistive manganite perovskite $La_{2/3}Ca_{1/3}MnO_3$ in a similar metathesis reaction

$$2/3LiMnO_2 + 1/3Li_2MnO_3 + 2/3LaOCl + 1/3CaCl_2 \rightarrow \\ La_{2/3}Ca_{1/3}MnO_3 + 4/3LiCl \quad (5)$$

where the final product, obtained at 850 °C in air, is single-phase (Fig. 3c) having the expected orthorhombic (*Pbnm*) perovskite structure[26] with $a = 5.473(2)$, $b = 7.734(2)$ and $c = 5.466(1)$ Å.

Next we investigated the synthesis of $AMnO_3$ (A = Ca, Sr, Ba) perovskites. For this purpose, we have chosen Li_2MnO_3 and ACl_2 (A = Ca, Sr, Ba) as reaction partners in the metathesis

$$Li_2MnO_3 + ACl_2 \rightarrow 2LiCl + AMnO_3 \text{ (A = Ca, Sr, Ba)} \quad (6)$$

The reaction occurs smoothly in air between 800–850 °C yielding the expected Mn(IV) perovskite oxides. Powder XRD patterns (Fig. 4) of the washed products clearly show that while $CaMnO_3$ is formed in the orthorhombic (*Pnma*) structure,[27] $SrMnO_3$ and $BaMnO_3$ are formed in the 4H and 2H hexagonal perovskite polytypic structures (Table 1) as expected. We have refined the powder XRD data of $BaMnO_3$ using the 2H polytypic structure as the model.[28] The refinement (Fig. 5) indeed shows that the sample we obtained in metathesis is

phase-pure and the crystallographic parameters (Table 2) are in agreement with the data reported[28] for $BaMnO_3$.

By employing a similar strategy, we have synthesized the perovskite titanates in the metathesis reaction

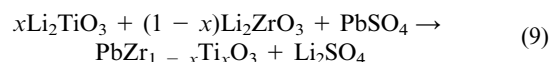$$Li_2TiO_3 + ACl_2 \rightarrow 2LiCl + ATiO_3 \text{ (A = Ca, Sr, Ba)} \quad (7)$$

Powder XRD patterns (Fig. 6) show that $CaTiO_3$, $SrTiO_3$ and $BaTiO_3$ are phase-pure materials and the lattice parameters obtained by the least squares refinement of the powder XRD data are in agreement with the values reported in the literature (Table 1). We have also carried out Rietveld refinement of the structure of $BaTiO_3$ from powder XRD data (Fig. 7). The crystallographic parameters obtained from the refinement (Table 3) are in agreement with the data reported for tetragonal (*P4/mmm*) $BaTiO_3$ in the literature.[29]

Our attempts to synthesize $PbTiO_3$ and $PbZrO_3$ similarly using $PbCl_2$ in reaction (7) did not yield the desired product. We could however synthesize the lead perovskites successfully using $PbSO_4$ (Fig. 8). The refinement of the structure of $PbTiO_3$ from powder XRD data is shown in Fig. 9a. It is likely that the low melting point of $PbCl_2$ (501 °C) and its instability at the reaction temperature (~ 800 °C) preclude the formation of $PbTiO_3$ and $PbZrO_3$, when $PbCl_2$ is used in the metathesis with Li_2TiO_3. $PbSO_4$ has recently been employed[6] in the synthesis of $PbZrO_3/ASO_4$ composites by the metathesis reaction

$$AZrO_3 + PbSO_4 \rightarrow PbZrO_3 + ASO_4 \text{ (A = Ca, Sr, Ba)} \quad (8)$$

We have also synthesized the well-known ferroelectrics, $PbZr_{1 - x}Ti_xO_3$ ($x \sim 0.5$; PZT) by the metathesis route,

$$xLi_2TiO_3 + (1 - x)Li_2ZrO_3 + PbSO_4 \rightarrow \\ PbZr_{1 - x}Ti_xO_3 + Li_2SO_4 \quad (9)$$

The reaction proceeds smoothly to completion at 850 °C/6 h yielding the PZT phases. We have synthesized two compositions with $x = 0.50$ and 0.52. While the $x = 0.50$ product has the rhombohedral (*R3m*) phase as the major component with tetragonal (*P4mm*) phase as the minor component (Fig. 8), Rietveld refinement of the powder XRD data for the $x = 0.52$ product showed it to be a 90 : 10 mixture of tetragonal :
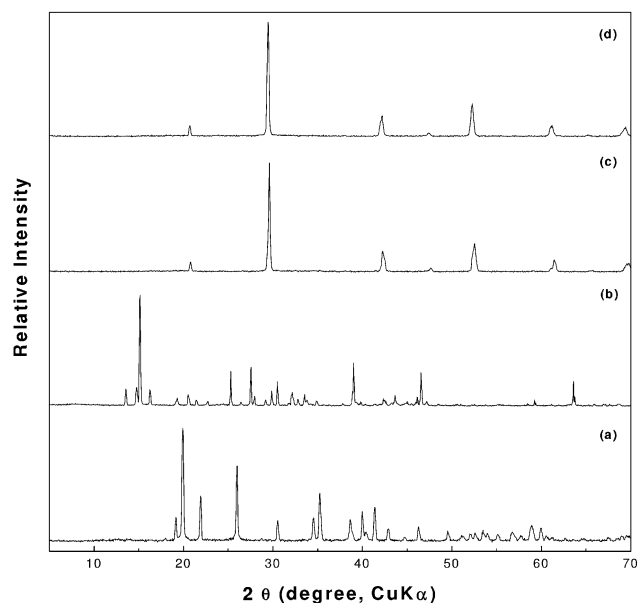

Fig. 11 Powder XRD patterns of (a) Li_2PbO_3, (b) $Ba(OH)_2.8H_2O$, (c) $BaPbO_3$ and (d) $BaPb_{0.75}Bi_{0.25}O_3$.

Table 5 Thermodynamic data[a] for metathesis reactions

Reaction	ΔH^0_{298} /kJ mol^{-1}	ΔS^0_{298} /kJ mol^{-1}	ΔG^0_{298} /kJ mol^{-1}	ΔH^0_{1100} /kJ mol^{-1}	ΔS^0_{1100} /kJ mol^{-1}	ΔG^0_{1100} /kJ mol^{-1}
Li_2TiO_3 (s) + $PbSO_4$ (s) → $PbTiO_3$ (s) + Li_2SO_4 (s)	−40.30	−0.015	−35.95	−16.78	+0.017	−35.34
Li_2ZrO_3 (s) + $PbSO_4$ (s) → $PbZrO_3$ (s)[b] + Li_2SO_4 (s)	−74.20	−0.002	−73.60	−59.03	+0.018	−78.75
Li_2TiO_3 (s) + $BaCl_2$ (s) → $BaTiO_3$ (s) + 2LiCl (s/l)[c]	+65.40	+0.013	+61.44	+108.59	+0.067	+34.85
Li_2TiO_3 (s) + $SrCl_2$ (s) → $SrTiO_3$ (s) + 2LiCl (s/l)[c]	+12.70	+0.02	+6.62	+44.40	+0.06	−21.46

[a] ΔH^0_{1100} and S^0_{1100} were calculated using the expressions, $\Delta H^0_T = \Delta H^0_{298} + {}_{298}\!\int^T C_P^0 dT$ and $S^0_T = S^0_{298} + {}_{298}\!\int^T (C_P^0/T)dT$, together with the expression for C_P^0 as a function of T where $T = 1100$ K(ref. 34). ΔG^0_{1100} values were calculated by using the expression $\Delta G^0_{1100} = \Delta H^0_{1100} - T\Delta S^0_{1100}$. [b] ΔH^0_{298}, S^0_{298} and C_P^0 values were taken from refs. 35 and 36. [c] For ΔH^0_{298}, S^0_{298} and ΔG^0_{298}, data for LiCl (s) was used. For ΔH^0_{1100}, S^0_{1100} and ΔG^0_{1100}, data for LiCl (l) was used.

rhombohedral PZT phases (Fig. 9b). Crystallographic parameters obtained from the refinement (Table 4) are in agreement with the data reported in the literature[30] for tetragonal and rhombohedral PZT. SEM images of $PbTiO_3$, $PbZrO_3$ and $PbZr_{0.48}Ti_{0.52}O_3$ (Fig. 10) show that the products are in the submicron range with a loose interconnectivity. We believe the synthesis of PZT solid solutions by the metathesis route is significant, in the light of the difficulties[31] involved (evaporation of PbO and control of cation stoichiometry) in the synthesis of these materials by the high temperature route. There has been considerable effort in recent times to develop alternate low temperature sol–gel routes for the synthesis of PZT materials.[5,31,32] Compared to the sol–gel routes, our method yields the desired product in a one-step reaction at relatively low temperatures ($\sim$850 °C) and short duration.

Having succeeded in the synthesis of several transition metal perovskite oxides of current interest by the metathesis route, we explored the possibility of synthesizing the metallic $BaPbO_3$ and its superconducting analogue $BaPb_{1-x}Bi_xO_3$. We envisaged that a metathesis between Li_2PbO_3 and $BaCl_2$ would yield $BaPbO_3$ perovskite in the reaction

$$Li_2PbO_3 + BaCl_2 \rightarrow BaPbO_3 + 2LiCl \qquad (10)$$

However, investigation of reaction (10) at various temperatures (600–900 °C) and durations (6–24 h) did not yield the desired product. Replacing $BaCl_2$ with $BaSO_4$ in reaction (10) was also unsuccessful. Nevertheless, we have been able to synthesize pure $BaPbO_3$ in the reaction between Li_2PbO_3 and $Ba(OH)_2\cdot8H_2O$. The reaction proceeds smoothly at a considerably low temperature (500 °C) to form $BaPbO_3$. We could also synthesize the superconducting $BaPb_{0.75}Bi_{0.25}O_3$ starting from $Li_2Pb_{0.75}Bi_{0.25}O_3$ and $Ba(OH)_2\cdot8H_2O$. The XRD patterns (Fig. 11) of the washed products show that they are single-phase, free from starting materials. The lattice parameters (a = 4.274(1) Å for $BaPbO_3$ and a = 4.285(2) Å for $BaPb_{0.75}Bi_{0.25}O_3$) obtained from least squares refinement of powder XRD data of the products are in agreement with the data reported in the literature.[33]

Finally, to probe into the driving force for the metathesis reactions reported here, we have calculated the enthalpy (ΔH) and free energy changes (ΔG) associated with a few of the reactions. For this purpose, we have used the thermodynamic data given in refs. 34–36. Our results given in Table 5 clearly show that the enthalpy change is indeed the driving force for the metathesis involving the formation of Li_2SO_4. However, for the cases involving LiCl as the product, the enthalpy data are unfavourable for metathesis. But the fact that these metatheses also occur smoothly (Table 1) suggests that other factors, such as volatilization of the alkali halide, could be involved in driving the reactions forward to yield the metathesis products. Further work is essential to establish the thermodynamic basis of metathesis reactions reported here.

Conclusions

In conclusion, we have shown that metathesis reactions starting from lithium containing rocksalt oxides provide a convenient route for the synthesis of a variety of perovskite oxides of current interest. Not only could we synthesize $LaCoO_3$, $LaMnO_3$, $AMnO_3$ and $ATiO_3$ (A = Ca, Sr, Ba) perovskite oxides in the reaction between the rocksalt oxide and metal oxychloride/chloride precursors, but we could also synthesize, by the same method, technologically important $La_{2/3}Ca_{1/3}MnO_3$ as well as PZT compositions in the $PbTiO_3$–$PbZrO_3$ system. Synthesis of Pb-containing perovskites however requires the use of $PbSO_4$ in the reaction. Finally, the metathesis approach could also be adapted for the synthesis of $BaPbO_3$ and its superconducting analogue $BaPb_{1-x}Bi_xO_3$ by employing $Ba(OH)_2\cdot8H_2O$.

Acknowledgements

References

1 P. A. Salvador, T-D. Doan, B. Mercey and B. Raveau, *Chem. Mater.*, 1998, **31**, 2592.
2 R. I. Walton, *Chem. Soc. Rev.*, 2002, **31**, 230.
3 J. Spooren, A. Rumplecker, F. Millange and R. I. Walton, *Chem. Mater.*, 2003, **15**, 1401.
4 S. O'Brien, L. Brus and C. B. Murray, *J. Am. Chem. Soc.*, 2001, **123**, 12085.
5 C. Liu, B. Zou, A. J. Rondinone and Z. J. Zhang, *J. Am. Chem. Soc.*, 2001, **123**, 4344.
6 M. Panda, R. Seshadri and J. Gopalakrishnan, *Chem. Mater.*, 2003, **15**, 1554.
7 A. A. Galkin, B. G. Kostyuk, V. V. Lunin and M. Poliakoff, *Angew. Chem., Int. Ed.*, 2000, **39**, 2738.
8 J. B. Wiley and R. B. Kaner, *Science*, 1992, **255**, 1093.
9 E. G. Gillan and R. B. Kaner, *Chem. Mater.*, 1996, **8**, 333.
10 I. P. Parkin, *Chem. Soc. Rev.*, 1996, **25**, 199.
11 K. Gibson, M. Ströbele, B. Blaschkowski, J. Glaser, M. Weisser, R. Srinivasan, H.-J. Kolb and H.-J. Meyer, *Z. Anorg. Allg. Chem.*, 2003, **629**, 1863.
12 J. Gopalakrishnan, T. Sivakumar, K. Ramesha, V. Thangadurai and G. N. Subbanna, *J. Am. Chem. Soc.*, 2000, **122**, 6237.
13 T. Sivakumar, R. Seshadri and J. Gopalakrishnan, *J. Am. Chem. Soc.*, 2001, **123**, 11496.
14 T. K. Mandal, N. Y. Vasanthacharya and J. Gopalakrishnan, *J. Mater. Chem.*, 2002, **12**, 635.
15 T. A. Hewston and B. L. Chamberland, *J. Phys. Chem. Solids*, 1987, **48**, 97.
16 G. C. Mather, C. Dussarrat, J. Etourneau and A. R. West, *J. Mater. Chem.*, 2000, **10**, 2219.
17 V. G. Lang, *Z. Anorg. Allg. Chem.*, 1954, **276**, 77.
18 V. G. Dittrich and R. Hoppe, *Z. Anorg. Allg. Chem.*, 1969, **371**, 306.

19 Y. Paik, C. P. Grey, C. S. Johnson, J.-S. Kim and M. M. Thackeray, *Chem. Mater.*, 2002, **14**, 5109.
20 L. H. Brixner and E. P. Moore, *Acta Crystallogr., Sect. C*, 1983, **39**, 1316.
21 W. Losocha and K. Lewinski, *J. Appl. Crystallogr.*, 1994, **27**, 437.
22 J. Rodríguez-Carvajal, *Physica B*, 1993, **192**, 55.
23 D. C. Harris and T. L. Hewston, *J. Solid State Chem.*, 1987, **69**, 182.
24 B. C. Hauback, H. Fjellvåg and N. Sakai, *J. Solid State Chem.*, 1996, **124**, 43.
25 J. Rodríguez-Carvajal, M. Hennion, F. Moussa, A. H. Moudden, L. Pinsard and A. Revcolevschi, *Phys. Rev. B*, 1998, **57**, R3189.
26 M. C. Sánchez, J. Blasco, J. García, J. Stankiewicz, J. M. De Teresa and M. R. Ibarra, *J. Solid State Chem.*, 1998, **138**, 226.
27 K. R. Poeppelmeier, M. E. Leonowicz, J. C. Scanlon, J. M. Longo and W. B. Yelon, *J. Solid State Chem.*, 1982, **45**, 71.

28 A. N. Christensen and G. Ollivier, *J. Solid State Chem.*, 1972, **4**, 131.
29 G. H. Kwei, A. C. Lawson, S. J. L. Billinge and S.-W. Cheong, *J. Phys. Chem.*, 1993, **97**, 2368.
30 J. Joseph, T. M. Vimala, V. Sivasubramanian and V. R. K. Murthy, *J. Mater. Sci.*, 2000, **35**, 1571.
31 J.-H. Choy and Y.-S. Han, *J. Mater. Chem.*, 1997, **7**, 1815.
32 J.-H. Choy, Y.-S. Han and S.-J. Kim, *J. Mater. Chem.*, 1997, **7**, 1807.
33 A. W. Sleight, J. L. Gillson and P. E. Bierstedt, *Solid State Commun.*, 1975, **17**, 27.
34 M. Binnewies and E. Milke, *Thermochemical Data of Elements and Compounds*, Second Edition, Wiley-VCH, Weinheim, 2002.
35 M. V. Rane, A. Navrotsky and G. A. Rossetti, Jr., *J. Solid State Chem.*, 2001, **161**, 402.
36 M. M. Lencka and R. E. Riman, *Thermochim. Acta*, 1995, **256**, 193.